Charge Recombination in Organic Photovoltaic Devices with High Open-Circuit Voltages

ARTICLE *in* JOURNAL OF THE AMERICAN CHEMICAL SOCIETY · OCTOBER 2008

Impact Factor: 12.11 · DOI: 10.1021/ja803054g · Source: PubMed

8 AUTHORS, INCLUDING:

Sebastian Westenhoff
University of Gothenburg
38 PUBLICATIONS **1,504** CITATIONS
SEE PROFILE

Ian A Howard
Karlsruhe Institute of Technology
51 PUBLICATIONS **2,193** CITATIONS
SEE PROFILE

Kiril Kirov
Eight19 Ltd
17 PUBLICATIONS **627** CITATIONS
SEE PROFILE

Hugo Bronstein
University College London
44 PUBLICATIONS **1,749** CITATIONS
SEE PROFILE

J|A|C|S
ARTICLES

Charge Recombination in Organic Photovoltaic Devices with High Open-Circuit Voltages

Sebastian Westenhoff,*[,†,‡] Ian A. Howard,[†] Justin M. Hodgkiss,[†] Kiril R. Kirov,[†] Hugo A. Bronstein,[§] Charlotte K. Williams,[§] Neil C. Greenham,[†] and Richard H. Friend*[,†]

OE-Group, Cavendish Laboratory, JJ Thomson Avenue, Cambridge CB3 0HE, U.K., Department of Chemistry, Biochemistry & Biophysics, University of Gothenburg, Box 462, 40530 Gothenburg, Sweden, and Department of Chemistry, Imperial College London, London SW7 2AZ, U.K.

Received May 9, 2008; E-mail: westenho@chem.gu.se; rhf10@cam.ac.uk

Abstract: A detailed charge recombination mechanism is presented for organic photovoltaic devices with a high open-circuit voltage. In a binary blend comprised of polyfluorene copolymers, the performance-limiting process is found to be the efficient recombination of tightly bound charge pairs into neutral triplet excitons. We arrive at this conclusion using optical transient absorption (TA) spectroscopy with visible and IR probes and over seven decades of time resolution. By resolving the polarization of the TA signal, we track the movement of polaronic states generated at the heterojunction not only in time but also in space. It is found that the photogenerated charge pairs are remarkably immobile at the heterojunction during their lifetime. The charge pairs are shown to be subject to efficient intersystem crossing and terminally recombine into F8BT triplet excitons within ~40 ns. Long-range charge separation competes rather unfavorably with intersystem crossing – 75% of all charge pairs decay into triplet excitons. Triplet exciton states are thermodynamically accessible in polymer solar cells with high open circuit voltage, and we therefore suggest this loss mechanism to be general. We discuss guidelines for the design of the next generation of organic photovoltaic materials where separating the metastable interfacial charge pairs within ~40 ns is paramount.

Organic semiconductor heterojunction solar cells are promising candidates for low-cost solar cell devices.[1−5] The active layer is a partially demixed blend of organic semiconducting materials, where the offsets between the conduction band-edges and valence band-edges are used to ionize photogenerated excitations at the heterojunction. Provided that the maximum phase size is of the order of the exciton diffusion length, excitons can be split across heterojunctions with near unit efficiency, even with minimal band-edge offsets.[1,2,6] Currently, the most efficient devices are made from blends with high electron affinity materials, such as fullerene derivatives.[3−5] In these blends, large band-edge offsets reduce the available open-circuit voltage and fundamentally limit the photovoltaic efficiency.[7] It is therefore surprising that material combinations with low band-edge offsets have so far failed to outperform the solar cells made from fullerene derivatives, despite the efficient quenching of excitons by charge transfer.[6] This suggests that a fundamental, performance-limiting process facilitates efficient recombination of charges in these blends.

A lively debate has developed to account for the efficiency limitation of charge collection. On one hand, inefficient bulk charge transport and the convoluted nature of charge-collection pathways are thought to lead to (trap-limited) *nongeminate* recombination as the dominant loss channel,[8] particularly when long ($>\mu$s) time scales are investigated by optical spectroscopy or electrical methods.[9,10] On the other hand, a number of studies that quantitatively account for all photogenerated charges suggest that intensity-independent *geminate* recombination may significantly deplete the number of long-lived and extractable charges.[6,11−14] The recent discovery of emission from tightly bound interfacial charge transfer states in blends of conjugated polymers has challenged the assumption that free charge pairs,

[†] Cavendish Laboratory.
[‡] Present address: University of Gothenburg.
[§] Imperial College London.

(1) Yu, G.; Gao, J.; Hummelen, J. C.; Wudl, F.; Heeger, A. J. *Science* **1995**, *270* (5243), 1789–1791.
(2) Halls, J. J. M.; Walsh, C. A.; Greenham, N. C.; Marseglia, E. A.; Friend, R. H.; Moratti, S. C.; Holmes, A. B. *Nature* **1995**, *376* (6540), 498–500.
(3) Brabec, C. J.; Sariciftci, N. S.; Hummelen, J. C. *Adv. Funct. Mater.* **2001**, *11* (1), 15–26.
(4) Kim, J. Y.; Lee, K.; Coates, N. E.; Moses, D.; Nguyen, T. Q.; Dante, M.; Heeger, A. J. *Science* **2007**, *317* (5835), 222–225.
(5) Peet, J.; Kim, J. Y.; Coates, N. E.; Ma, W. L.; Moses, D.; Heeger, A. J.; Bazan, G. C. *Nat. Mater.* **2007**, *6* (7), 497–500.
(6) McNeill, C. R.; Westenhoff, S.; Groves, C.; Friend, R. H.; Greenham, N. C. *J. Phys. Chem. C* **2007**, *111* (57), 19153–19160.
(7) Koster, L. J. A.; Mihailetchi, V. D.; Blom, P. W. M. *Appl. Phys. Lett.* **2006**, *88* (9), 093511-1–093511-3.
(8) Nelson, J. *Phys. Rev. B* **2003**, *67* (15), 155209.
(9) Kim, Y.; Cook, S.; Tuladhar, S. M.; Choulis, S. A.; Nelson, J.; Durrant, J. R.; Bradley, D. D. C.; Giles, M.; McCulloch, I.; Ha, C. S.; Ree, M. *Nat. Mater.* **2006**, *5* (3), 197–203.
(10) Montanari, I.; Nogueira, A. F.; Nelson, J.; Durrant, J. R.; Winder, C.; Loi, M. A.; Sariciftci, N. S.; Brabec, C. *Appl. Phys. Lett.* **2002**, *81* (16), 3001–3003.
(11) Mihailetchi, V. D.; Koster, L. J. A.; Hummelen, J. C.; Blom, P. W. M. *Phys. Rev. Lett.* **2004**, *93* (21), 216601.
(12) Offermans, T.; Meskers, S. C. J.; Janssen, R. A. J. *J. Chem. Phys.* **2003**, *119* (20), 10924–10929.

10.1021/ja803054g CCC: $40.75
Published on Web 09/18/2008

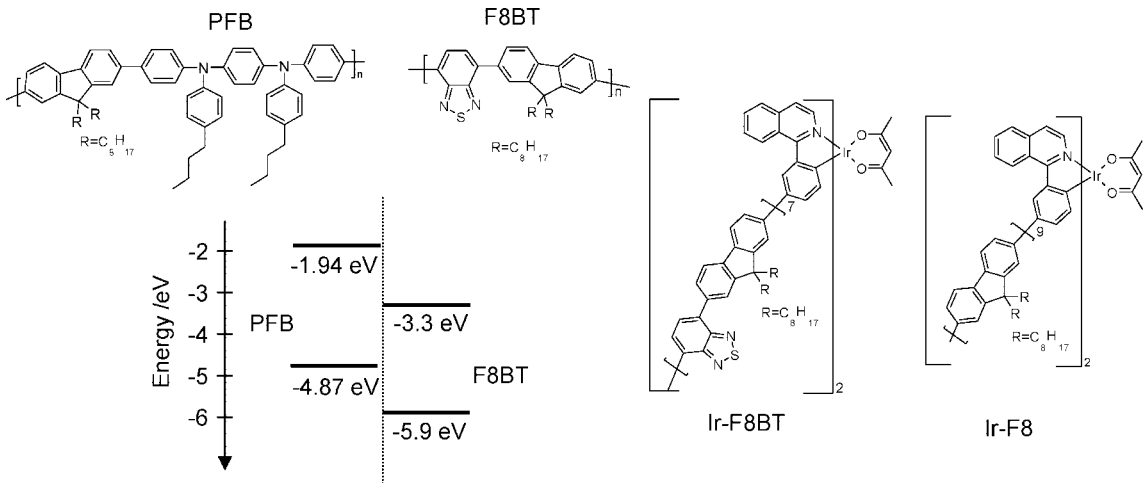

Figure 1. Chemical structures and energy of excited states: The chemical structures of PFB and F8BT are shown together with their highest occupied molecular orbital (HOMO) and lowest unoccupied molecular orbital (LUMO) energies. The HOMO level was deduced from cyclic voltammetry and the LUMO level was calculated based on the HOMO level and the $\pi-\pi^*$ gap. The chemical structure of [iridium(III) bis(1-(3′-(ω-(4‴,4‴,5‴,5‴-tetramethyl-1″,3″,2″-dioxaborolan-2″-yl)-oligo[9″,9″-dioctylfluorene-alt-benzothiadiazole)phenyl)isoquinolinato-*N*,*C*′)(acetyl acetonate)] (Ir−F8BT) and [Ir(III)bis(1-(3′-(ω-bromo-oligo[9″,9″-dioctylfluoren-2″,7″-diyl])phenyl)isoquinolinato-*N*,*C*)(acetylacetonate)] (Ir−F8) are also displayed.

which are electrons and holes without any wave function overlap, are the inevitable product of exciton quenching at the heterojunction.[15,16] Furthermore, spectroscopic investigations of blends with low band-edge offsets have shown that triplet excitons are formed with high yields.[17−19] However, the exact loss mechanism is not clear, mainly because electrical measurements lack time resolution to probe the early (ns) time scales, and it remains challenging to directly obtain spatial information about charge separation from the transient optical spectra of polymer-based polarons and excitons.

To investigate the performance-limiting recombination process in low band-edge offset photovoltaic devices, we introduce polarization-resolved transient absorption (TA) spectroscopy to directly track the movement of photogenerated charges. This measurement takes advantage of three features of bulk heterojunction organic solar cells: i) Electronic states probed by TA spectroscopy are predominantly polarized uniaxially along the chain segments on which they reside; ii) many excitons are ionized in close proximity to the site of photon absorption, thus propagating polarization information to the primary interfacial charge pair; and iii) in amorphous materials, spatial motion of transient states is associated with loss of polarization anisotropy.[20,21] We observe that most photoexcitations never form fully separated charges but that they remain as tightly bound and immobile charge pairs at the heterojunction. We combine these measurements with visible and infrared TA data spanning over seven decades in time, supported by an independent spectroscopic assignment of triplet states, to show that 75% of the immobile charge pairs undergo intersystem crossing and recombine terminally into triplet excitons on a 40 ns time scale. This approach should prove valuable to assess the viability of new materials engineered to favor long-range charge separation.

Results and Discussion

In our study, we investigate blends of polyfluorene copolymers poly(9,9-dioctylfluorene-*co*-bis-*N*,*N*′-(4,butylphenyl)-bis-*N*,*N*′-phenyl-1,4-phenylene-diamine) (PFB) and poly(9,9-dioctylfluorene-*alt*-benzothiadiazole) (F8BT) (Figure 1). The films were spin cast from chloroform solution, to produce intimately mixed blends, with phase sizes of less than 10 nm.[6,22] Time-resolved optical TA spectra for pure F8BT and the blend containing 50% F8BT are summarized in parts a and b of Figure 2, respectively. We note that 490 nm excitation is used to selectively excite the low-bandgap material F8BT ($\lambda_{max} = 460$ nm) over PFB ($\lambda_{max} = 385$ nm). In both samples, we observe a positive $\Delta T/T$ signal for wavelengths shorter than 620 nm and a negative signal for longer wavelengths at a delay time of 350 fs. These features have been assigned to excitonic stimulated emission and photoinduced absorption of F8BT, respectively.[23] At a delay time of 900 ps, no signal is detected for the pure F8BT sample, whereas the TA spectrum of the blend is dominated by a secondary, spectrally broad absorption. This has been assigned to electrons and holes generated at the heterojunction.[22,23] We report elsewhere that the charge generation time is limited by diffusion of excitons to the heterojunction and charge generation is completed at ∼200 and ∼10 ps for the blends containing 50% and 10% F8BT, respectively.[22] Excitons are split with a very high efficiency despite only a ∼200 meV stabilization of the charge-transfer state relative to the exciton energy.[15]

(13) De, S.; Pascher, T.; Maiti, M.; Jespersen, K. G.; Kesti, T.; Zhang, F. L.; Inganas, O.; Yartsev, A.; Sundstrom, V. *J. Am. Chem. Soc.* **2007**, *129* (27), 8466–8472.
(14) Marsh, R. A.; Groves, C.; Greenham, N. C. *J. Appl. Phys.* **2007**, *101* (8), 083509.
(15) Morteani, A. C.; Dhoot, A. S.; Kim, J. S.; Silva, C.; Greenham, N. C.; Murphy, C.; Moons, E.; Cina, S.; Burroughes, J. H.; Friend, R. H. *Adv. Mater.* **2003**, *15* (20), 1708–1712.
(16) Offermans, T.; van Hal, P. A.; Meskers, S. C. J.; Koetse, M. M.; Janssen, R. A. J. *Phys. Rev. B* **2005**, *72* (4), 045213.
(17) Ford, T. A.; Avilov, I.; Beljonne, D.; Greenham, N. C. *Phys. Rev. B* **2005**, *71* (12), 125212.
(18) Veldman, D.; Bastiaansen, J.; Langeveld-Voss, B. M. W.; Sweelssen, J.; Koetse, M. M.; Meskers, S. C. J.; Janssen, R. A. J. *Thin Solid Films* **2006**, *511*, 581–586.
(19) Ford, T. A.; Ohkita, H.; Cook, S.; Durrant, J. R.; Greenham, N. C. *Chem. Phys. Lett.* **2008**, 237–241.
(20) Grage, M. M. L.; Pullerits, T.; Ruseckas, A.; Theander, M.; Inganäs, O.; Sundström, V. *Chem. Phys. Lett.* **2001**, *339* (1−2), 96–102.
(21) Westenhoff, S.; Beenken, W. J. D.; Friend, R. H.; Greenham, N. C.; Yartsev, A.; Sundström, V. *Phys. Rev. Lett.* **2006**, *97* (16), 166804.
(22) Westenhoff, S.; Howard, I. A.; Friend, R. H. *Phys. Rev. Lett.* **2008**, *101*, 016102.
(23) Stevens, M. A.; Silva, C.; Russell, D. M.; Friend, R. H. *Phys. Rev. B* **2001**, *63* (16), 165213.

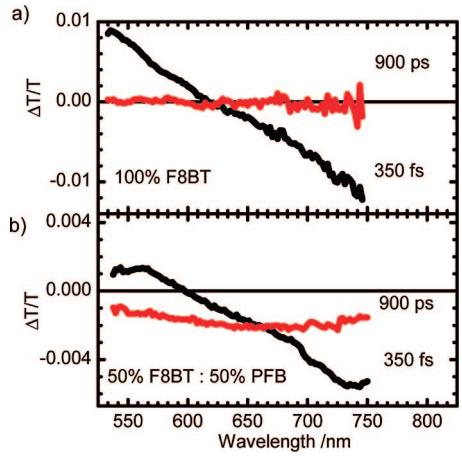

Figure 2. Transient absorption spectroscopy of PFB:F8BT on a femto- to nanosecond time scale: Panels (a) and (b) show the transient transmission spectra of F8BT and 50% PFB:50% F8BT, respectively. The delay times of the spectra were integrated over ±150 fs and ±100 ps for the 350 fs and 900 ps spectra, respectively. Excitation was at 490 nm with a fluence of $\sim 3 \times 10^{13}$ photons/cm^2.

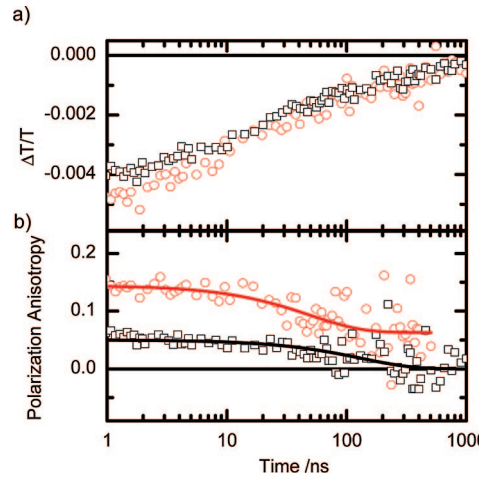

Figure 3. Polarization resolved transient absorption spectroscopy on nano- to microsecond time scale: Panel (a) shows the differential transmission kinetics recorded at 532 nm probe wavelength generated by the second harmonic of the Nd:YVO_4 laser for the two blend ratios with the polarization set to the magic angle to measure the population dynamics. Red open circles and black squares correspond to the blend containing 10% and 50% F8BT, respectively. The excitation fluence was 1×10^{14} and 1×10^{13} at 490 nm, respectively. Panel (b) shows the corresponding polarization anisotropy decays with color coding as in panel (a). The lines are monoexponential fits as a guide to the eye.

To resolve the fate of the charge pairs on longer time scales, we augmented our femtosecond TA spectrometer with a Nd:YVO_4 laser, Q-switched via an electronically delayed trigger. With this setup, TA can be performed on the nanosecond to millisecond time scales. We simultaneously measured differential absorption signals for parallel and perpendicular polarizations of a single-wavelength probe, yielding both time-resolved polarization anisotropy ($r = (\Delta T/T^{para} - \Delta T/T^{perp})/(\Delta T/T^{para} + 2\,\Delta T/T^{perp})$) and magic-angle (population) decays ($\Delta T/T^{para} + 2\,\Delta T/T^{perp}$).[24] We recall that the magnitude and decay dynamics of the polarization anisotropy measures the migration of photoexcitations within the disordered polymer films.

Part a of Figure 3 shows the population decay kinetics of the blends containing 50% (red circles) and 10% F8BT (black squares), measured with a probe wavelength of 532 nm. At this wavelength, mainly charged excitations are probed (vide infra). The similarity of the two kinetics traces suggests that their decay dynamics are insensitive to the blend composition. Nevertheless, the polarization anisotropy kinetics, shown in part b of Figure 3, reveals considerable differences between the two blends. First, the anisotropy is higher for the blend with 10% F8BT (r(1 ns) $\sim$ 0.16) compared to 50% F8BT (r(1 ns) $\sim$ 0.06). This is in agreement with a diffusion limited charge generation mechanism.[22] In the 50% blend, excitons created within the F8BT domain have a longer mean path length to reach a heterojunction, and thus a lower level of polarization anisotropy at the time of charge transfer. Second, the polarization anisotropy of the blends containing 10% F8BT does not decay to zero. This is interpreted to arise from the small size of F8BT domains in this blend ratio, constraining the orientational freedom of transient states residing therein. Importantly, the signal retains significant polarization anisotropy on a time scale exceeding tens of nanoseconds in both blends. This shows conclusively that charge pairs are immobile at the heterojunction for a considerably long time. Indeed, the fact that this time scale approaches or exceeds that of the charge population decay (part a of Figure 3) leads us to the conclusion that most charge pairs must remain at the site of generation until ultimately recombining there geminately.

We continued our investigation by measuring nanosecond TA spectra using a broad-band probe pulse (spanning from 530 to 780 nm) to identify any other states that may participate in the signal evolution. Part a of Figure 4 shows that the spectrum of the F8BT:PFB blend at 5 ns (red circles) resembles the shape of the 900 ps spectrum in part b of Figure 2, assigned to charge pairs. Inspecting the blend spectrum at 75 ns (black squares) reveals a spectral shift, with a new component absorbing in the >700 nm region. We assign this component (vida infra) to F8BT triplet excitons, which are known to be generated in significant yields in this blend.[17] The triplet formation process has been suggested to occur on submicrosecond time scales, but the exact formation dynamics have proved difficult to distinguish from those of charged states.[19]

To unambiguously verify the TA spectral shape of F8BT triplet excitons, we use an F8BT derivative (Ir−F8BT) bearing an iridium moiety (Ir−piq, Figure 1) conjugated with the oligomer backbone (details of the synthesis are provided in the Supporting Information). The large spin−orbit coupling induced by the iridium atom ensures facile intersystem crossing. Photoexcitations transfer to the triplet level on the F8BT unit with ~100% efficiency because it is the excited-state with lowest energy (energy diagram in part a of Figure 5), and charge-transfer intermediate states are avoided. Consequently, no photoluminescence is observed from either the F8BT or Ir−piq chromophores of Ir−F8BT (part b of Figure 5). The photophysical model depicted in part a of Figure 5 is confirmed by the photoluminescence measurements of the related poly-(9,9′-dioctyl-fluorene) (F8) based oligomer, Ir−F8.[25] In this case, the F8 triplet exciton is raised due to its larger bandgap compared to F8BT, and the triplet level on the Ir−piq subunit becomes the lowest energy level

(24) Westenhoff, S.; Daniel, C.; Friend, R. H.; Silva, C.; Sundström, V.; Yartsev, A. *J. Chem. Phys.* **2005**, *122* (9), 094903.

(25) Bronstein, H. A.; Finlayson, C. E.; Kirov, K. R.; Friend, R. H.; Williams, C. K. *Organometallics* **2008**, *24* (13), 2980–2989.

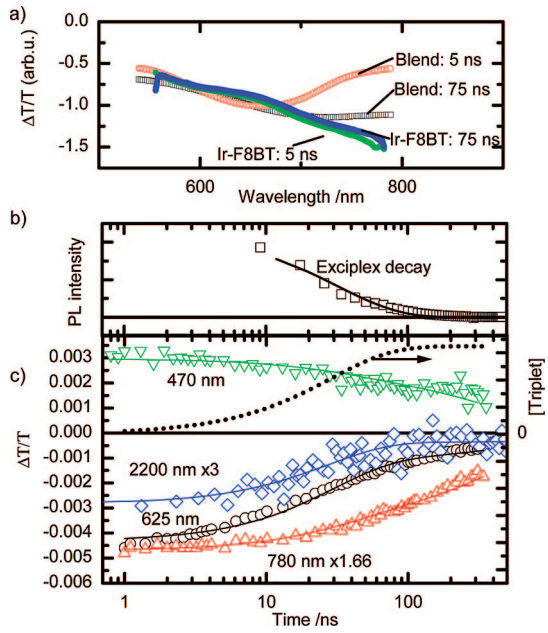

Figure 4. Triplet generation in F8BT:PFB polymer blends: Panel (a) shows time-resolved spectra of a PFB:F8BT (50%/50%) blend and Ir−F8BT films at delay times as indicated in the figure. The spectra are smoothed using a fast Fourier transform filter (Origin 6.0, Originlabs Inc.). Panel (b) shows the photoluminescence decay of the exciplex as measured by time-correlated single-photon counting at 650 nm (symbols) together with a monoexponential fit (line). Panel (c) shows TA kinetics with magic angle polarization between pump and probe at wavelengths as indicated in the figure. Excitation was at 355 nm with fluences of $\sim 5 \times 10^{13}$ photons/cm^2 (at 650 nm, 775 nm, and 2200 nm probe wavelength), and $\sim 2.5 \times 10^{13}$ photons/cm^2 (at 475 nm probe wavelength). The dashed black line is the triplet density reconstructed from the global fit.

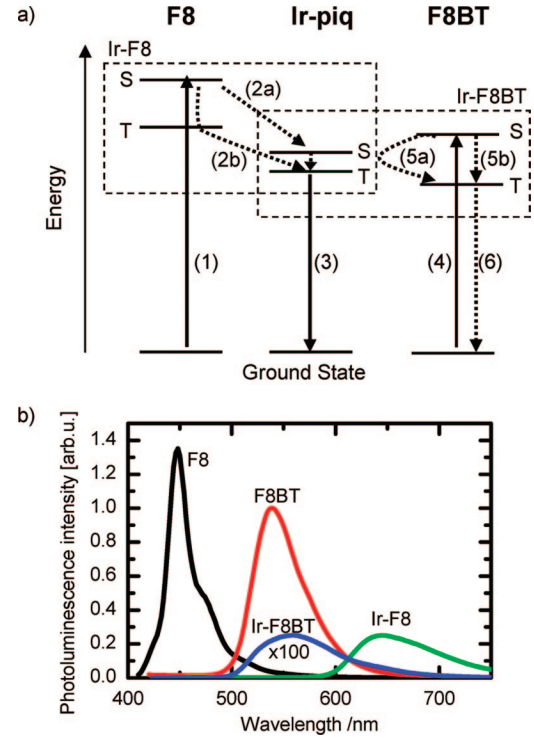

Figure 5. Photophysics of the iridium−oligofluorene copolymers: Panel (a) shows the energy scheme for the lowest-lying excited singlet (S) and triplet (T) states of F8BT, Ir−piq and F8. The singlet−triplet splitting of the charge-transfer excitations in Ir−piq is expected to be much smaller than for F8 and F8BT. The relevant energy levels of the oligomers Ir−F8 and Ir−F8BT are indicated by the boxes. In the photocycle of Ir−F8, (1) light is absorbed to create a singlet exciton on the F8 moiety, (2a) energy transfers to Ir−piq, where efficient intersystem crossing may occur or (2b) triplet excitons are formed on F8 by intersystem crossing and subsequently transfer to the Ir−piq triplet level, and (3) deactivation is by phosphorescence from Ir−piq. In the case of Ir−F8BT, the photocycle involves (4) absorption of light to form singlet excitons on F8BT, (5a) energy transfer to Ir−piq, efficient intersystem crossing, and back transfer to the F8BT triplet exciton or alternatively (5b) enhanced intersystem crossing on F8BT directly, and (6) deactivation by internal conversion. Panel (b) shows the photoluminescence spectra of F8, F8BT, Ir−F8BT, and Ir−F8. The spectra are corrected for the spectral response function of the detector. The integral of the spectra are scaled according to the photoluminescence quantum yield, which were measured using an integrating sphere.

in the Ir−F8 system. Consequently, strongly red-shifted phosphorescence from the Ir−piq moiety is observed (part b of Figure 5). The spectral signature of triplet excitons in Ir−F8BT is further confirmed by the observation that the TA spectra of the iridium-sensitized F8BT analogue exhibit no spectral shift with decay time (green and blue triangles shown in part a of Figure 4). Importantly, the spectral shapes of the TA spectrum of Ir−F8BT and the delayed TA spectrum of the blends are very similar, which strongly supports our assignment of triplet exciton formation in the blends.

The generation of triplet excitons from charge pairs represents a potential limitation to photovoltaic efficiencies in polymer solar cells. However, the yield of free charge carriers is dependent on the competitive kinetics of long-range charge separation versus recombination. To quantify the branching of primary charge pairs, we have measured the time dependence of the TA signals at the following wavelengths: i) 475 nm (probing the ground-state bleach of F8BT and thus the total number of excited states), ii) 625 nm (probing mainly the photoinduced absorption of polarons), iii) 780 nm (probing the photoinduced absorption of polarons and triplets in F8BT), and iv) 2200 nm (below the bandgap of triplet excitons and thus exclusively probing the photoinduced absorption of polarons[26]) (part c of Figure 4). Care was taken to use the same excitation fluence and wavelength ($\lambda_{exc} = 355$ nm) in all measurements. Importantly, the data at the infrared (IR) wavelength shows that most of the charges decay on a nanosecond time scale. Triplets are generated on the same time scale as indicated by the dotted line in part c of Figure 4. This confirms that triplet excitons are formed directly from the charge-transfer state. However, ~10% of the IR signal prevails beyond 500 ns, thus we conclude that some charges do not undergo conversion into triplets. As the polarization anisotropy has clearly decayed to zero in the 50% blend at 500 ns delay time (part b of Figure 3), we conclude that at this time the remaining charge pairs must have migrated away from the heterojunction.

On the basis of our observations we propose the photophysical model depicted in Figure 6. Primary interfacial charge pairs (CP) are generated on a picosecond time scale with near unit efficiency.[22] The anisotropy measurements (part b of Figure 3) show that these are trapped at the heterojunction. The charge pairs may be emissive exciplexes[15] that can decay directly to the ground state (GS), or nonemissive polaron pairs.[27] All interfacial charge pairs may decay into triplet excitons (*T*), which

(26) Sheng, C. X.; Tong, M.; Singh, S.; Vardeny, Z. V. *Phys. Rev. B* **2007**, *75* (8), 085206.

(27) Huang, Y.-S.; Westenhoff, S.; Avilov, I.; Sreearunothai, P.; Hodgkiss, J. M.; Deleener, C.; Friend, R. H.; Beljonne, D. *Nat. Mater.* **2008**, *7*, 483–489.

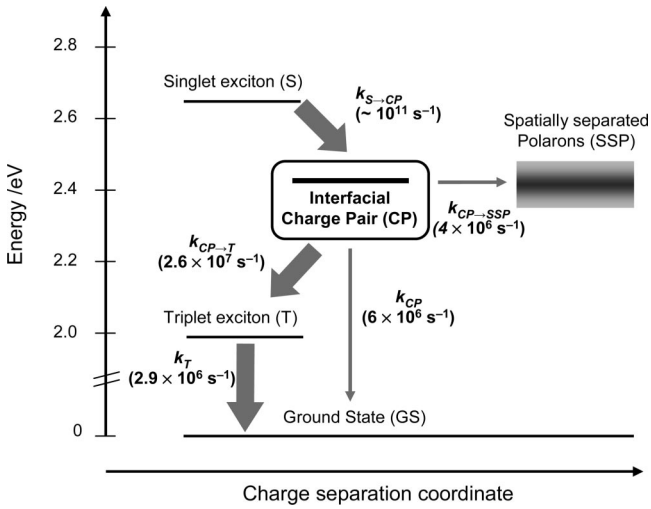

Figure 6. Charge recombination mechanism at the polymer−polymer heterojunction: The energy of the interfacial charge pair and F8BT triplet exciton were taken to be 200 meV (ref 15) and 700 meV (ref 28) below the F8BT singlet exciton energy level, respectively. The bold arrows summarize the main flow of energy.

are thermodynamically available for blend systems with small band edge offsets[18] and high singlet−triplet exchange energies typical of conjugated polymers,[28] or further charge separate into spatially separated polarons (SSP). We have assumed that the excited-state absorptions due to interfacial and separated charge pairs are indistinguishable and that the bleaching cross section is similar for triplet, singlet, and charged excitations. The rate equations for the states are: $d[CP]/dt = -k_{CP\rightarrow T}[CP] - k_{CP}[CP] - k_{CP\rightarrow SSP}[CP]$, $d[T]/dt = k_{CP\rightarrow T}[CP] - k_T[T]$, $d[SSP]/dt = k_{CP\rightarrow SSP}[CP]$, and $d[GS]/dt = k_T[T] + k_{CP}[CP] + k_{SSP}[SSP]$. We fit the TA data globally based on these rate equations (see Methods for details) and require $k_{CP\rightarrow T} + k_{CP\rightarrow SSP} + k_{CP} = 3.5 \times 10^7$ s^{-1}, which is the decay constant of the exciplex photoluminescence (part b of Figure 4). We do not include the decay of the spatially separated polarons in the model, as the relatively small signal from SSP states does not allow us to extract the decay dynamics of this state. We have confirmed that no significant correlation between the parameters exists (Supporting Information). The fit allows us to determine the branching ratios between the three decay channels of interfacial charge-pair state without any further a priori assumptions about the density or cross sections of the states involved. The rate constants yielded are $k_{CP\rightarrow T} = (2.6 \pm 0.4) \times 10^7$ s^{-1}, $k_{CP} = (6 \pm 4) \times 10^6 s^{-1}$, and $k_{CP\rightarrow SSP} = (4 \pm 0.8) \times 10^6$ s^{-1}. We note that the intersystem crossing rate from the charge-transfer state ($k_{CP\rightarrow T}$) is similar to rates of triplet formation from singlet excitons in pristine F8BT, which was estimated to be 1.2×10^7 s^{-1}.[17] Thus, the increased triplet population in blends is due to the increased lifetime of the charge-transfer state relative to a singlet exciton in a pristine polymer film.

We conclude that immobile, metastable interfacial states are the bottleneck of device efficiency in blends of F8BT and PFB. Seventy-five percent of these charge pairs recombine at the place of their formation into triplet excitons on a time scale of ~40 ns. The extractable charges are constrained by a modest 10% geminate pair dissociation yield. This readily explains the modest external quantum efficiency of 3.4% measured in solar cells under short circuit conditions made from this material system.[6] The clear implication is that unless open-circuit voltage is sacrificed to make the triplet exciton thermodynamically inaccessible, interfacial charge pairs are vulnerable to terminal loss as triplets if they are not further separated within ~40 ns.

Subject to the time-scale constraint imposed by triplet formation, facilitating rapid geminate pair dissociation in organic photovoltaic devices calls for strategies to direct charge transport vectorially away from the interface in opposition to their mutual Coulombic attraction. Nature overcomes a similar kinetic quandary in photosynthesis, where photoexcited electrons are rapidly shuttled away from holes via a cascade of quinone acceptors with appropriately positioned energy levels.[29] Likewise, dye-sensitized solar cells owe their impressive quantum efficiency in part to an architecture in which the electron donor and acceptor materials are bridged by a sensitizer to direct charge carriers in opposite directions over a longer length-scale.[30] Whereas neither of these examples are optimized with respect to voltage retention, they may yet provide inspiration for heterojunctions engineered to favor long-range charge separation. Current state-of-the-art bulk heterojunction photovoltaic devices comprise blends of P3HT and PCBM.[5] Here, the charge pairs are stable with respect to triplet excitons (leading to modest open-circuit voltages of ~0.6 V).[31] Notwithstanding, recent experimental evidence suggests that the high performance of PCBM:polymer solar cells could be due to kinetic rather than energetic considerations; with its high local charge mobility allowing charges to readily escape the interface region on a picosecond-to-nanosecond time scale with minimal applied field.[32,33] This consideration suggests that electron acceptors with lower electron affinities than PCBM ought still to be considered for photovoltaic devices, as long as they exhibit high local electron mobilities. The intersystem crossing time of ~40 ns sets a general benchmark against which the kinetics of long-range charge separation must be favorable for efficient charge extraction in the next generation of photovoltaic materials. Polarization-resolved, nanosecond time-resolved TA spectroscopy should prove valuable for directly assessing the interfacial kinetic control in new bulk-heterojunction device architectures.

Methods

Transient Absorption Spectroscopy. Femto- to picosecond TA spectroscopy was performed utilizing two optical paramagnetic amplifiers (OPAs) seeded by the 800 nm output (pulse duration <80 fs) of a commercially available oscillator/amplifier system (Tsunami and Spitfire Pro, Spectra Physics). Narrow-band pulses were generated using a TOPAS system (Light Conversion). Broad-band pulses spanning from 530 to 800 nm were generated with a home-built non-collinear OPA (Manzoni, C.; Polli, D.; Cerullo, G. *Rev. Sci. Instrum.* **2006**, *77*, 023103). Differential transient transmission spectra were measured by spectrally resolving probe and reference pulses in a spectrograph and recording the light intensity with two diode arrays. The 256 pixel array (S3901256Q, Hamamatsu) was read out using

(28) Wilson, J. S.; Dhoot, A. S.; Seeley, A.; Khan, M. S.; Kohler, A.; Friend, R. H. *Nature* **2001**, *413* (6858), 828–831.
(29) Wraight, C. A. *Photochem. Photobiol.* **1979**, *30* (6), 767–776.
(30) O'Regan, B.; Gratzel, M. *Nature* **1991**, *353* (6346), 737–740.
(31) Ohkita, H.; Cook, S.; Astuti, Y.; Duffy, W.; Heeney, M.; Tierney, S.; McCulloch, I.; Bradley, D. D. C.; Durrant, J. R. *Chem. Commun.* **2006**, (37), 3939–3941.
(32) Barbour, L. W.; Hegadorn, M.; Asbury, J. B. *J. Phys. Chem. B* **2006**, *110* (48), 24281–24286.
(33) Marsh, R. A.; McNeill, C. R.; Abrusci, A.; Campbell, A. R.; Friend, R. H. *Nano Lett.* **2008**, *8* (5), 1393–1398.

Table 1. Fitting Parameters

parameter	cross sections			
probe wavelength	475 nm	650 nm	780 nm	2200 nm
$\sigma_{CP}{}^{a}$ /10^{-16} cm^2	–	4.3 ± 0.2	2.8 ± 0.1	1 ± 0.1
$\sigma_{T}{}^{a}$ /10^{-16} cm^2	–	1.1 ± 0.3	1.8 ± 0.4	–
$\sigma_{abs}{}^{a}$ /10^{-16} cm^2	4.0 ± 0.3	–	–	–

parameter	rates
$k_{CP\rightarrow T}{}^{b}$ /10^7 s^{-1}	2.6 ± 0.4
$k_{CP}{}^{b}$ /10^6 s^{-1}	6 ± 4
$k_{CP\rightarrow SSP}{}^{b}$ /10^6 s^{-1}	4 ± 0.8
k_T/10^6 s^{-1}	2.9 ± 0.6

[a] The cross sections are referenced to the absorption cross section of F8BT at 475 nm, which was determined to be $\sigma_{abs} = 4 \times 10^{-16}$ cm^{-2} in ref 23 [b] $k_{CP\rightarrow T} + k_{CP} + k_{CP\rightarrow SSP} = 3.5 \times 10^{-7}$ s^{-1} was required during fitting. The value was determined as the monoexponential lifetime of the delayed exciplex emission.

a commercially available circuit at 2 MFz (C7844, Hamamatsu) and digitized on the fly for each laser pulse using a PXI-6122 card (National Instruments). The transmission with excitation light on and off was calculated using a computer with a real-time operating system (PXI-8175 and Labview real-time) and recorded as a function of optical delay between pump and probe. With this detection system, a complete TA spectrum can be recorded from two subsequent laser pulses. The time-resolved spectra shown in this paper were averaged over several hundred laser shots. They were corrected for chirp of the probe, and offsets at negative time were substracted. The time resolution was ~120 fs, as judged from the rise time of the signal.

For nanosecond- to microsecond TA spectroscopy, a Q-switched Nd:YVO_4 laser (AOT-YVO-25QSPX, Advanced Optical Technology Ltd.) with a pulse length of 500 ps was synchronized electronically with the Ti:Sapphire femtosecond laser by means of a variable delay generator (DG 535, Stanford Research Systems). The instrument response was ~0.8 ns, as judged by the rise time of the signal, and the observation window was <1 ms and was limited only by the repetition rate of the femtosecond laser. The second (532 nm) and third (355 nm) harmonic of the Nd:YVO_4 laser was used as either a pump or a single-wavelength probe source. For polarization anisotropy measurements, we separated *s* and *p* polarizations with a cube polarizer and detected the $\Delta T/T$ signals with polarization parallel and perpendicular to the excitation source simultaneously.[24]

Global Fitting Procedure According to the Photophysical Model (Figure 6). The integrated rate laws for the model are

$$[\mathrm{CP}] = [\mathrm{CP}]_0 \exp(-(k_{\mathrm{CP}\rightarrow\mathrm{SSP}} + k_{\mathrm{CP}} + k_{\mathrm{CP}\rightarrow T})t) \quad (1)$$

$$[T] = [\mathrm{CP}]_0 \frac{k_{\mathrm{CP}\rightarrow T}}{k_{\mathrm{CP}} + k_{\mathrm{CP}\rightarrow\mathrm{SSP}} + k_{\mathrm{CP}\rightarrow\mathrm{T}}} (1 - [\mathrm{CP}]) \exp(-k_T t) \quad (2)$$

$$[\mathrm{SSP}] = [\mathrm{CP}]_0 \frac{k_{\mathrm{CP}\rightarrow\mathrm{SSP}}}{k_{\mathrm{CP}} + k_{\mathrm{CP}\rightarrow\mathrm{SSP}} + k_{\mathrm{CP}\rightarrow T}} (1 - [\mathrm{CP}]) \quad (3)$$

And the total differential absorption signal is given by

$$\Delta T/T = [-\sigma_{CP}([\mathrm{CP}] + [\mathrm{SSP}]) - \sigma_T[T] + \sigma_{\mathrm{abs}}([\mathrm{CP}] + [T] + [\mathrm{SSP}])]d \quad (4)$$

with *d* as the film thickness, σ_{CP}, σ_T, and σ_{abs} respectively being the cross section of the charged excitations (which is assumed to be the same for interfacial charge pairs and spatially separated polarons), cross section of the F8BT triplet excitons, and the absorption cross section of F8BT. See Figure 6 for other assignments. The fitting parameters are summarized in Table 1. The errors were determined by a dependency analysis (Supporting Information).

Acknowledgment. The authors acknowledge financial support from EPSRC. H.A.B. and C.K.W. acknowledge EPSRC grant EP/C548132/1. S.W. thanks Fitzwilliam College Cambridge for a Junior Research Fellowship, and I.A.H. thanks the Cambridge Commonwealth Trust for financial support.

Supporting Information Available: Statistical analysis of the TA global fitting parameters and the synthesis of Ir−F8BT. This material is available free of charge via the Internet at http://pubs.acs.org.

JA803054G